Output and Power Characteristics of LLC Resonant DC-DC Converters for Photovoltaic Applications

Georgi Petrov Terziyski[1] and Svetla Dimitrova Lekova[2]

[1]*University of Food Technologies - Plovdiv, 26 Maritsa blvd., 4000 Plovdiv, Bulgaria*

[2]*University of Chemical Technology and Metallurgy - Sofia, 1784 Sofia, Bulgaria*

Abstract. The output and power characteristics of different LLC resonant DC-DC converter configurations are obtained, which will inform the designer of the resonant converters, what is the type of LLC configuration, respectively the type of resonant circuit at a specific frequency distortion. In addition, for some of the LLC configurations under consideration, an output voltage higher than the power supply is obtained, and for them are plotted the curves of the maximum power point (MPP), indicating at what coordinates of the output voltage and output current, the converter under consideration (PV) will have maximum power.

Keywords: LLC resonant DC-DC converters, photovoltaic applications.

1. INTRODUCTION

Photovoltaic modules (PV modules) are one of the most promising trends in the modern energetics. They belong to the so-called renewable energy sources, which are finding a wider use in households and businesses. The main reason for this is the use of solar energy and its transformation in a voltage that can be used either for personal consumption or for sale to energy distributors. It is a must that PV modules will be maximized which leads to increase of the efficiency of the used resonant converter. Many authors (Eötvös et al, 2010; Rani et al, 2016; Seyezhai et al, 2013; Shvaraja, 2015; Sridhar et al, 2016; Thamaraimanalan, 2015) recommend the use of resonant converters using in its resonant circuit a LLC configuration. The converters with third-line resonant circuits (Batarseh, 1994; Yang, 2003) are most often preferred since they can operate over the full range of idle to short circuit while preserving the soft commutation conditions of the inverter's controllable switches. In (Eötvös et al, 2010; Rani et al, 2016; Seyezhai et al, 2013; Shvaraja, 2015; Sridhar et al, 2016; Thamaraimanalan, 2015), LLC resonant converters used in connection to photovoltaic (solar) panels are considered.

The purpose of the present work is to obtain the output and power characteristics of different kinds of configurations of LLC resonant DC-DC converters that will give information to the designer of the resonant converters what the LLC configuration is, respectively the resonant circuit at a specific distortion by frequency. In addition, to determine the maximum power point (MPP) for those configurations of LLC converters for which an output voltage is higher than the power supply.

2. ANALYSIS OF THE CONVERTERS

The diagram of the converter under consideration is shown in Fig. 1. It consists of an inverter (controllable switches $S_1 \div S_4$ with reverse diodes $D_1 \div D_4$), a resonant tank, a matching transformer (Tr), a capacitive filter (C_F), and a load resistor (R_0).

Different configurations composed of LLC resonant tanks (Batarseh, 1994; Yang, 2003) are shown in Fig. 2.

For the purposes of the analysis it is assumed that all the elements in the diagram are ideal (no losses in them), the power devices switch from one state into another instantly, the matching transformer has a coefficient of transformation

equal to unity, and the pulsations of the supplying U_d and the output voltages U_0 are negligibly small. It is also assumed that according to the chosen method of analysis, only the first harmonics of the currents and voltages act in the circuit under consideration. The following notations are accepted (Bankov et al, 2009):

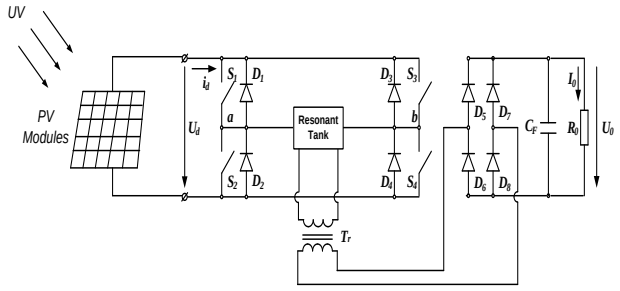

Fig. 1 PV Module with a resonant DC-DC converter with a capacitive output filter.

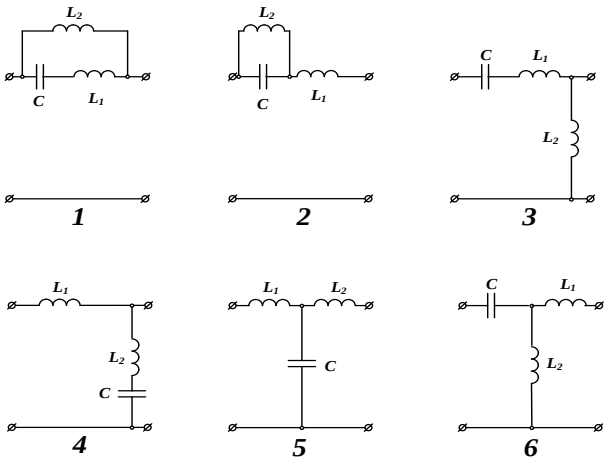

Fig 2 Configurations of LLC resonant tanks.

$U_0^{'} = U_0 / U_d$ - normalized output voltage;

$I_0^{'} = I_0 / \left(U_d / \rho_0\right)$ - normalized output current;

$I_d^{'} = I_d / \left(U_d / \rho_0\right)$ - normalized input current;

$R_0^{'} = R_0 / \rho_0 = U_0^{'} / I_0^{'}$ - normalized load parameter;

$\rho_0 = \sqrt{L_1 / C}$ - wave resistance of the oscillating circuit;

$P_0^{'} = U_0 I_0 / U_d^2 / \rho_0$ - normalized output power;

$\nu = \omega_s / \omega_0$ - frequency distortion of the oscillating circuit;

ω_s - operational frequency of the converter;

$\omega_0 = 1/\sqrt{L_1 C}$ - resonant frequency of the oscillating circuit;

$a = L_2 / L_1$ - inductive's ratio between the two inductivities in the oscillating circuit.

To show how the analysis was made, we will take a random resonant circuit – configuration No. 5 from Fig. 2.

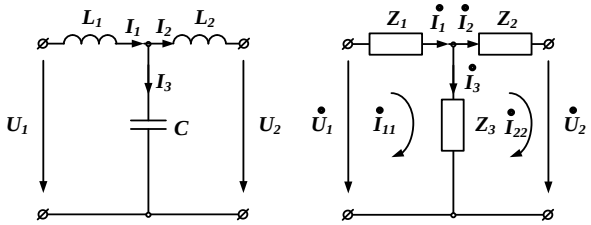

Fig. 3 Resonant tank for config. No. 5.

For simplicity, we assume that the two circuits are equivalent, then, according to the contour current method, we compile the following system of equations:

$$\begin{vmatrix} \left(Z_1 + Z_3\right)\dot{I}_{11} - Z_3\dot{I}_{22} = \dot{U}_1 \\ -Z_3\dot{I}_{22} + \left(Z_2 + Z_3\right)\dot{I}_{22} = -\dot{U}_2 \end{vmatrix} \quad (1)$$

After formal transformations, we express $\dot{U}_2$, i.e.

$$\dot{U}_2 = \frac{\dot{U}_1 Z_3 - \left(Z_1 Z_2 + Z_2 Z_3 + Z_3 Z_1\right)\dot{I}_{22}}{Z_1 + Z_3} \quad (2)$$

Let us replace the impedances of the coils and the capacitor from the resonant circuit with their equalities

$$\begin{aligned} Z_1 &= j\omega L_1 = j\nu\rho_0; \\ Z_2 &= j\omega L_2 = aZ_1 = j\nu\rho_0 a; \\ Z_3 &= 1/\ j\omega C = \rho_0 / j\nu; \end{aligned} \quad (3)$$

After substituting (3) into (2) and formal transformations we get:

$$\dot{U}_2 = \frac{\dot{U}_1}{1-\nu^2} + j\frac{\nu\rho_0 a\left(\nu^2 - 1\right)\dot{I}_{22} - \nu\rho_0\dot{I}_{22}}{1-\nu^2} \quad (4)$$

The vector diagram of the voltages from the resonant circuit is as follows:

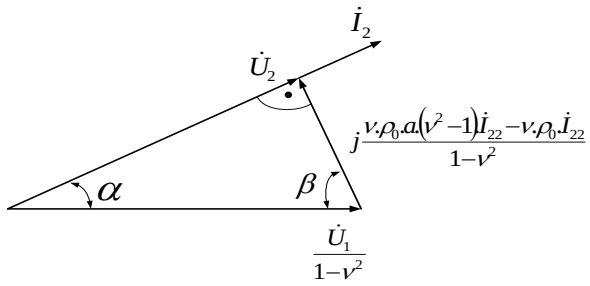

Fig. 4 Vector voltage diagram.

For the obtained rectangular triangle the Pythagorean theorem is in effect:

$$\dot{U}_2^2+\left[\frac{\nu\rho_0 a(\nu-1)\dot{I}_{22}-\nu\rho_0\dot{I}_{22}}{1-\nu^2}\right]^2=\frac{\dot{U}_1^2}{(1-\nu^2)^2} \quad (5)$$

After formal transformations we get (6):

$$\begin{aligned}&\dot{U}_2^2(1-\nu^2)^2+\nu^2\rho_0^2a^2(\nu^2-1)^2\dot{I}_{22}^2\\&-2\nu^2\rho_0^2a(\nu^2-1)^2\dot{I}_{22}^2+\nu^2\rho_0^2\dot{I}_{22}^2=\dot{U}_1^2\end{aligned} \quad (6)$$

where $$\dot{U}_1=\frac{2\sqrt{2}}{\pi}U_d \quad (7)$$

$$\dot{I}_{22}=\frac{\pi}{2\sqrt{2}}I_0$$

$$\dot{U}_2=\frac{2\sqrt{2}}{\pi}U_0$$

By substituting the dependencies (7) in (6) and formal transformations in relative units we get:

$$U_0^{'}=\sqrt{\frac{1-(\pi^4/64)\left[a\nu(\nu^2-1)-\nu\right]^2I_0^{'2}}{(1-\nu^2)}} \quad (8)$$

The last expression (8) gives the equation of the wanted output characteristics $U_0^{'}=f\left(I_0^{'},\nu,a\right)$.

The output power of the converter in relative units can be expressed from the equation for the output characteristics, after its multiplication by $I_0^{'}$:

$$P_0^{'}=\frac{I_0^{'}}{8(1-\nu^2)}\sqrt{64-\pi^4\left[a\nu(\nu^2-1)-\nu\right]^2I_0^{'2}} \quad (9)$$

With a set value of ν, the function $P_0^{'}=f\left(I_0^{'},\nu,a\right)$ has a maximum at

$$U_0^{'}=\frac{\sqrt{2}}{2(\nu^2-1)} \text{ and } I_0^{'}=\frac{4\sqrt{2}}{\pi^2\left[a\nu(\nu^2-1)-\nu\right]} \quad (10)$$

$$I_{0\max}^{'}=\frac{4}{\pi^2(\nu^2-1)\left[a\nu(\nu^2-1)-\nu\right]} \quad (11)$$

The relative resistance of the resistor in which it is distributed the maximum power is:

$$R_{0\max}^{'}=\frac{\pi^2\left[a\nu(\nu^2-1)-\nu\right]}{8(\nu^2-1)} \quad (12)$$

Output and Power characteristics of LLCconfigurations

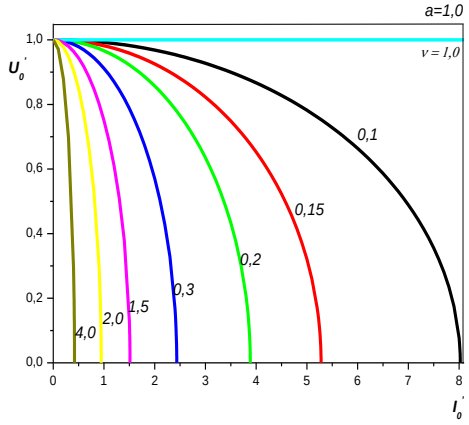

Fig. 5 Output characteristics for config. No 1.

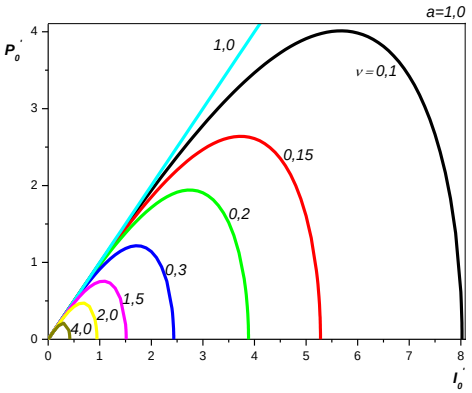

Fig. 6 Power characteristics for config. No. 1.

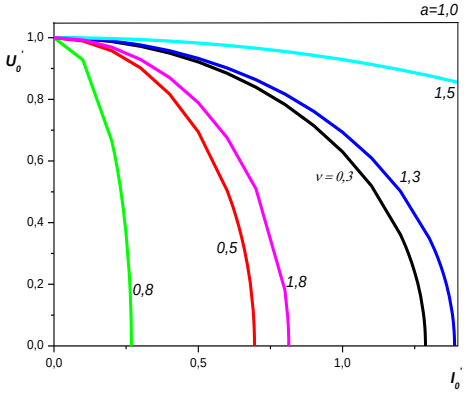

Fig. 7 Output characteristics for config. No. 2.

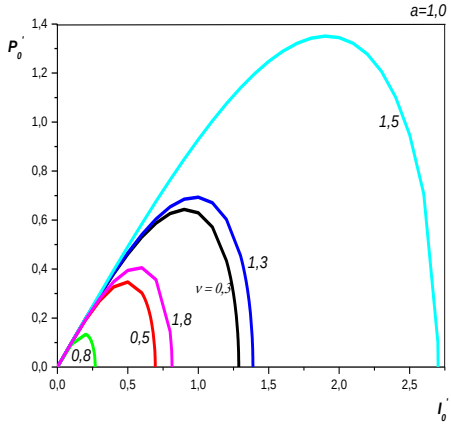

Fig. 8 Power characteristics for config. No. 2.

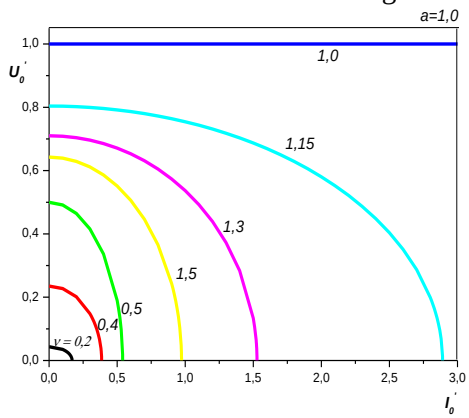

Fig. 9 Output characteristics for config. No. 3.

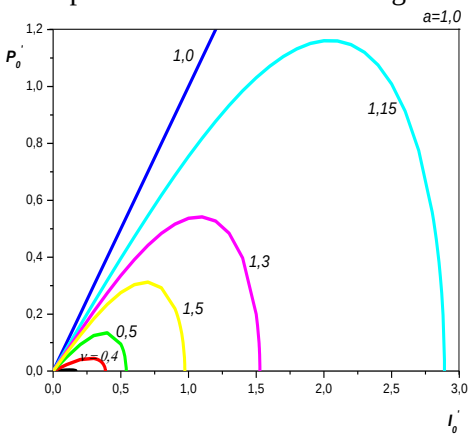

Fig. 10 Output characteristics for config. No. 2.

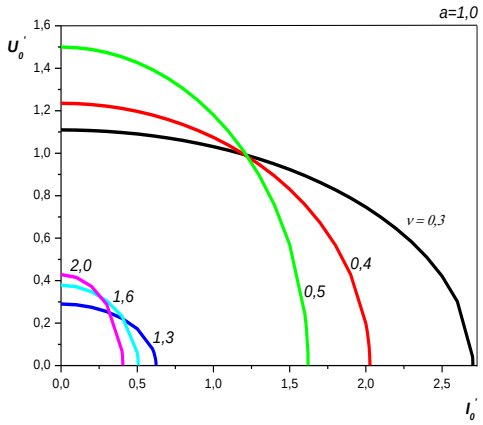

Fig. 11 Output characteristics for config. No 4.

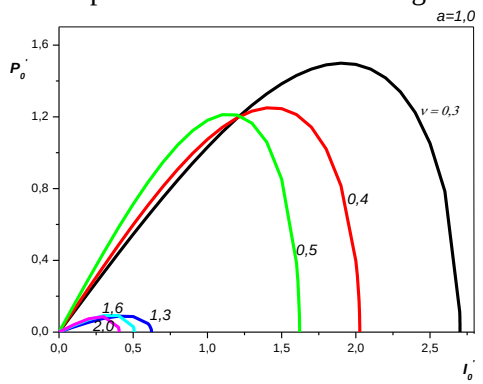

Fig. 12 Power characteristics for config. No. 4.

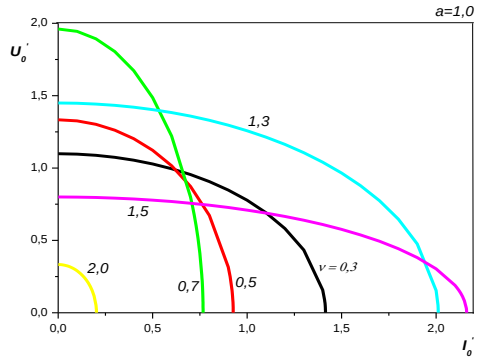

Fig. 13 Output characteristics for config. No. 5.

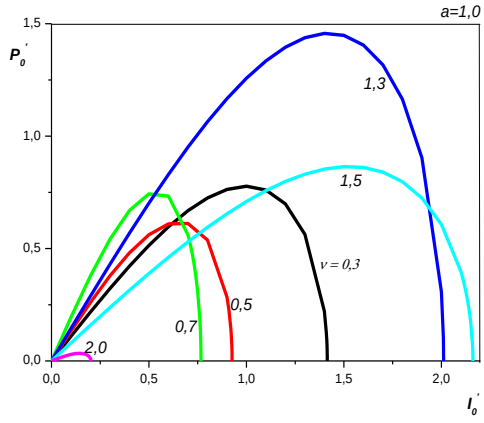

Fig. 14 Power characteristics for config. No. 5.

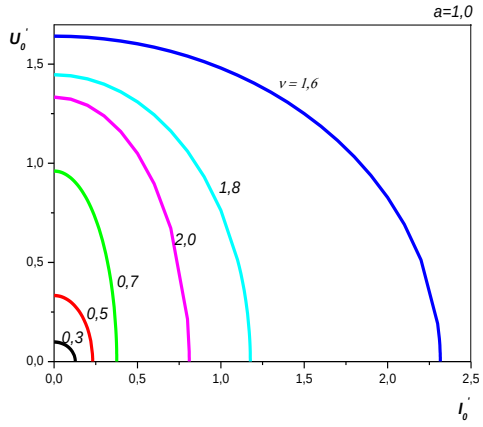

Fig. 15 Output characteristics for config. No. 6.

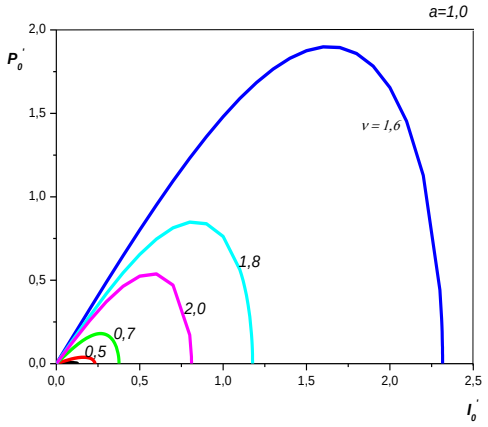

Fig. 16 Power characteristics for config. No 6.

3. ANALYSIS OF THE RESULTING CHARACTERISTICS

The resulting output characteristics for the LLC converter configurations under consideration indicate that the converter of Fig. 1 can operate as a voltage source or current source. When the converter acts as a voltage source, it resembles the use of photovoltaic (solar) panels, rechargeable batteries, managed or unmanaged rectifiers, impulse converters of DC voltage, etc. Conversely, when the converter operates as a current source, it resembles the use of a voltage source encompassed by a negative current feedback, a sequentially connected voltage source and throttle, for which purpose the impedance of the throttle has to be of considerable value, etc.

The output characteristics shown in Fig. 5 are positioned concentrically and show that when the converter operates at below and above its resonant frequency, with increasing of the operating frequency, the short-circuit current decreases and the idle voltage remains at a constant value. These are characteristics inherent to a voltage source limited by current.

The output characteristics shown in Fig. 7 are analogous to those shown in Fig. 5 for operation of the converter below its resonant frequency.

The output characteristics shown in Fig. 9 and Fig. 15 show that when the converter operates below its resonant frequency, the short-circuit current and idle voltage increase. These are characteristics that are located concentrically and are inherent in a current source, resistive to operation even with a short-circuit. When the converter operates above its resonant frequency with the increasing of the operating frequency, the short-circuit current and the idle voltage decrease.

The output characteristics shown in Fig. 11 and Fig. 13 show that when the converter operates below its resonant frequency with the increasing of the operating frequency, the short-circuit current decreases, but the idle voltage increases. These are characteristics that intersect and are inherent to a voltage source limited by current. The same conclusions apply to the output characteristics of Fig. 11 for the operation of the converter above its resonant frequency.

An area of operation can be noticed in some of the output characteristics, where the output voltage becomes higher than the supplying one, i.e., $U_0^{'} > 1$. It can be seen from figures 11, 13 and 15. For this reason, configurations 4, 5 and 6 of Fig. 2 are the most efficient and most preferred for building LLC resonant DC-DC converters for photovoltaic applications. In Fig. 17, 18 and 19 are shown the curves of the output power and voltage as a function of the output current for a fixed maximum power point (MPP), which determines the value of the output voltage and the current for a specified definite frequency distortion ν. From Fig. 17 shows that the resonant converter which is used, operates below its resonant frequency $\omega_s < \omega_0 (\nu = 0,3)$, whereby the controllable switches of the inverter will be clogged at zero

current, resulting in elimination of the clogging losses (ZCS).

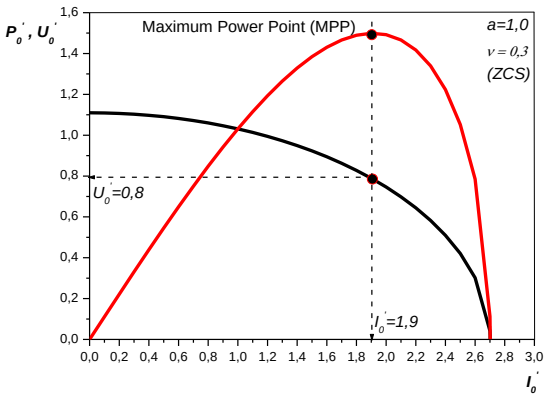

Fig. 17 Maximum power point curve for config. No. 4.

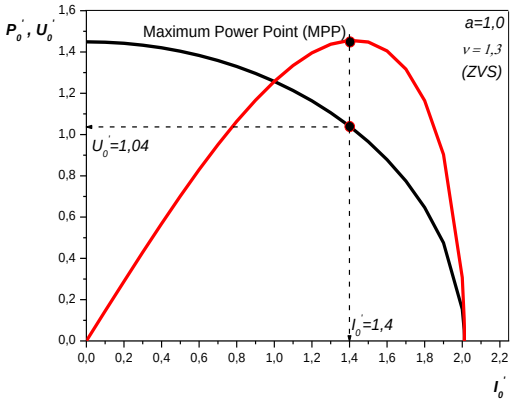

Fig. 18 Maximum power point curve for config. No. 5.

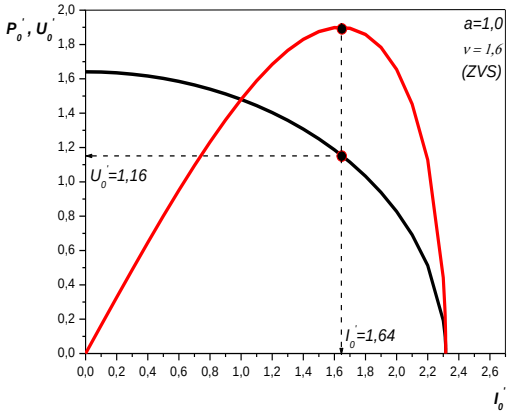

Fig. 19 Maximum power point curve for config. No. 6.

One of the ZCS approaches is by plugging the inductance sequentially into each of the controllable switches of the inverter. The sequentially connected inductance of each of the control switches ensures that when unlocked, the current through them will not increase by jump but smoothly, depending on the value of the inductance used.

From Fig. 18 and 19 shows that the resonance converter used operates over its resonance frequency $\omega_s > \omega_0 (\nu = 1{,}3)$, whereby the controllable switches of the inverter will be unlocked at zero voltage, resulting in elimination of the loss when they unlocked (ZVS).

To achieve zero voltage switching (ZVS), a capacitor of the appropriate capacitance is usually connected to each of the controllable switches of the inverter. Usually the IGBT transistor is the most common. Here the unlocking of the controllable switches of the capacitor is embedded in the controllable key itself, which switches at zero-voltage on them must be guaranteed by the operating principle of the control circuit used. Conversely, when the inverter controllable keys are clogged, the zero voltage on them is provided by the parallel-connected capacitor.

4. DESIGN OF LLC RESONANT DC-DC CONVERTER

When designing the resonant DC-DC converter, the following parameters are usually set: output power P_0, output voltage U_0 and operating frequency f (Bankov et al, 2009). Assuming that the efficiency of the inverter is equal to one, the parameters of the power source are:

$$U_d = \frac{U_0}{U_0^{'}} = \frac{U_0}{\sqrt{\frac{1-\left(\pi^4/64\right)\left[a\nu\left(\nu^2-1\right)-\nu\right]^2 I_0^{'2}}{\left(\nu^2-1\right)}}} \quad (13)$$

$$I_d = \frac{P_0}{U_d} = \frac{P_0\sqrt{\frac{1-\left(\pi^4/64\right)\left[a\nu\left(\nu^2-1\right)-\nu\right]^2 I_0^{'2}}{\left(\nu^2-1\right)}}}{U_0} \quad (14)$$

The values of the switching elements L_1, C and L_2 are determined by the expressions for

the maximum output power and the distortion of the resonant circuit:

$$P_0 = \frac{4}{\pi^2\left(\nu^2-1\right)\left[a\nu\left(\nu^2-1\right)-\nu\right]}\frac{U_d^2}{\sqrt{L_1/C}} \tag{15}$$

$$\nu = 2\pi f\sqrt{L_1 C} \tag{16}$$

Then for elements L_1, C and L_2 the dependencies are obtained:

$$L_1 = \frac{2\nu}{\pi^3\left(\nu^2-1\right)\left[a\nu\left(\nu^2-1\right)-\nu\right]}\frac{U_d^2}{fP_0} \tag{17}$$

$$C = \frac{\pi\nu\left(\nu^2-1\right)\left[a\nu\left(\nu^2-1\right)-\nu\right]}{8}\frac{P_0}{fU_d^2} \tag{18}$$

$$L_2 = aL_1\frac{2\nu a}{\pi^3\left(\nu^2-1\right)\left[a\nu\left(\nu^2-1\right)-\nu\right]}\frac{U_d^2}{fP_0} \tag{19}$$

Using the above methodology, the values of the most important parameters of the rated nominal mode of the proposed converter for photovoltaic applications have been calculated. The output data is as follows:

$P_0 = 15$ W; $f = 50$ kHz; $U_d = 17{,}5$ V; $\nu = 1{,}3$.

The following parameter values were obtained:

$$L_1 = L_2 = 123\ \mu\text{H};\ C = 139{,}06\ \text{nF};$$

$$U_0 = 18{,}2\ \text{V};\ I_0 = 0{,}822\ \text{A};\ R_0 = 22{,}141\ \Omega.$$

Using the OrCAD PSpice program, a computer simulation of the proposed converter was performed. In Fig. 20 shows the voltage circuits on the oscillating circuit, the current through the coil L_1, the current through the coil L_2, the voltage on the switching capacitor C and the voltage on the load resistor R_0.

There is a very good match between the results obtained from the numerical solution and the computer simulation. For example, the voltage on the load resistor R_0 obtained at the maximum photovoltaic power (see Fig. 18) is calculated with a relative error:

$$\delta_{U_{R_0}} = \frac{18{,}2-17{,}88}{17{,}88}.100\% = 1{,}79\%$$

The resulting 1,79 % relative error achieves a practical accuracy (error below 5 %). Therefore, the proposed design methodology is suitable for engineering calculations.

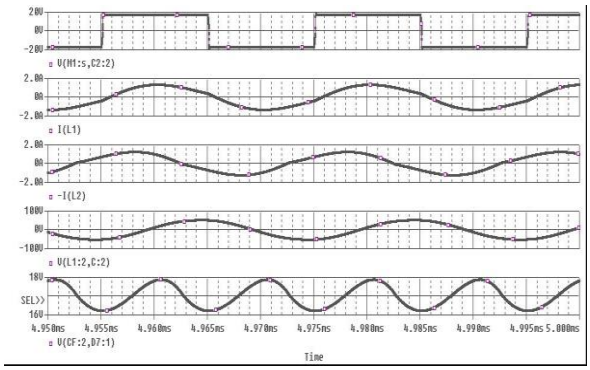

Fig. 20 The results of the computer simulation.

5. CONCLUSIONS

Output and Power characteristics of LLC resonant DC-DC converters for photovoltaic applications has been carried out by the method of the first harmonic. Their operation below and above the operating frequency has been investigated.

As a result from the analysis, the output and power characteristics for a number of configurations of LLC resonant tanks have been obtained. Depending on the operation of the converter below or above its resonant frequency, the resulting output characteristics indicate that the converter can operate as a voltage source or current source.

In some of the output characteristics, an area of operation can be seen in which the output voltage becomes higher than the supply voltage, i. e. $U_d^{'} > 1$. This can be seen in Figs. 11, 13 and 15. For this reason, configurations 4, 5 and 6 of Fig. 2 are the most efficient and most preferred for building LLC resonant DC-DC converters for photovoltaic applications. In Fig. 17, 18 and 19 are shown the power output and voltage curves as a function of the output current for a fixed maximum power point

(MPP), which determines the value of the output voltage and the current for an exactly definite distortion of the frequency ν.

The resulting output and power characteristics of this study (Fig. 5 to Fig. 16) give information to the designer of the resonant converters what kind of LLC configuration (resonant circuit) should be at an exactly definite distortion of the frequency.

The resulting curves (Fig. 17 to Fig. 19) will inform the designer and the user of a resonant converter accordingly, what should be the type of LLC configuration chosen to obtain an output voltage greater than the supply voltage, with a maximum power for an exactly define distortion of the frequency.

REFERENCES

Batarseh I., 1994. *Resonant Converter Topologies with Three and Four Energy Storage Elements*, IEEE Transactions on Power Electronics, Vol. 9, No. 1, pp. 64-73.

Buccela C., Cecati C., Latafat H. and Razi K., 1999. *Multi String Grid – Connected PV System with LLC Resonant DC/DC Converter*, Springer, Intell Ind Syst 1, pp. 37-49.

Eötvös E., Bodor M., 2010. *DC/DC resonant converter for PV system*, SCYR – 10th Scientific Conference of Young Researchers – FEI TU of Košice.

Rani K. and Rao C., 2016. *LLC Resonant Inverter for Solar PV Applications*, IJAECS, Vol. 3, Issue 2, pp. 128-132.

Seyezhai R., Ramathilagam G., Chitra P. and Vennila V., 2013. *Investigation of Half-Bridge LLC Resonant DC-DC Converter for Photovoltaic Applications*, IJIREEICE, Vol. 1, Issue 3, pp. 76-81.

Shivaraja L., 2018. *Modeling and Simulation of LLC Resonant Converter for Photovoltaic Systems*, IJETIE, Vol. I, Issue 4, pp. 175-179.

Sridhar S. and Naik V., 2016. *A ZVS Based Boost Resonant Converter for PV Applications*, IEEJ, Vol. 7, No. 4, pp. 2212-2222.

Thamaraimanalan V., 2015. *An Isolated Series Resonant Converter for PV Applications*, IRJETM, Vol. 1, Issue 3, pp. 01-04.

Yang B., 2003. *Topology Investigation for Front End DC/DC Power Conversion for Distributed Power System*, Dissertation, Virginia Polytechnic Institute, Blacksburg, pp. 247-307.

Bankov N., Terziyski G., Vuchev A. and Dinkov H., 2009. *Analysis of serial-parallel resonant DC/DC Converter using the first harmonic method*, Conference of Food Science, Engineering and Technologies, Vol. LVI, Issue 2, pp. 385-389 (in Bulgarian).

Bankov N., Terziyski G., Vuchev A. and Dinkov H., 2009. *Work characteristics and design of serial-parallel resonant DC/DC Converter*, Conference of Food Science, Engineering and Technologies, Vol. LVI, Issue 2, pp. 390-395 (in Bulgarian).